Environ. Eng. Res. 2019; 24(3): 376-381
https://doi.org/10.4491/eer.2018.083

pISSN 1226-1025
eISSN 2005-968X

A shell layer entrapping aerobic ammonia-oxidizing bacteria for autotrophic single-stage nitrogen removal

Hyokwan Bae[1†], Minkyu Choi[2]

[1]*Department of Civil and Environmental Engineering, Pusan National University, Busan 46241, Republic of Korea*
[2]*Center for Water Resource Cycle Research, Korea Institute of Science and Technology (KIST), Seoul 02792, Republic of Korea*

ABSTRACT

In this study, a poly(vinyl) alcohol/sodium alginate (PVA/SA) mixture was used to fabricate core-shell structured gel beads for autotrophic single-stage nitrogen removal (ASNR) using aerobic and anaerobic ammonia-oxidizing bacteria (AAOB and AnAOB, respectively). For stable ASNR process, the mechanical strength and oxygen penetration depth of the shell layer entrapping the AAOB are critical properties. The shell layer was constructed by an interfacial gelling reaction yielding thickness in the range of 2.01-3.63 mm, and a high PVA concentration of 12.5% resulted in the best mechanical strength of the shell layer. It was found that oxygen penetrated the shell layer at different depths depending on the PVA concentration, oxygen concentration in the bulk phase, and free ammonia concentration. The oxygen penetration depth was around 1,000 μm when 8.0 mg/L dissolved oxygen was supplied from the bulk phase. This study reveals that the shell layer effectively protects the AnAOB from oxygen inhibition under the aerobic conditions because of the respiratory activity of the AAOB.

Keywords: Autotrophic single-stage nitrogen removal, Core-shell structured gel bead, Free ammonia, Mechanical strength, Oxygen penetration depth, Poly(vinyl) alcohol/sodium alginate

1. Introduction

Compared to the nitrification and denitrification, combined partial nitritation (PN)-Anaerobic ammonium oxidation (ANAMMOX) is a cost-efficient biological nitrogen removal process. It reduces aeration costs by 57% (Eq. (1) and (2)) and eliminates the cost of organic carbon loading for heterotrophic denitrification because the ANAMMOX process is completely autotrophic (Eq. (3)). PN-ANAMMOX requires balanced activities of aerobic and anaerobic ammonia-oxidizing bacteria (AAOB and AnAOB, respectively). In a two-stage reactor configuration, aerobic pretreatment using AAOB performs the partial oxidation of ammonia to nitrite (Eq. (2)) to achieve a molar ratio of nitrite to ammonia of 1.32 according to the stoichiometric equation of the ANAMMOX reaction (Eq. (3)). In the second stage, AnAOB oxidize ammonia using nitrite as an electron acceptor and produce nitrogen gas and nitrate.

Full nitrification:

$$1\ NH_4^+ + 1.83\ O_2 + 1.97\ HCO_3^- \rightarrow 0.0244\ C_5H_7NO_2 + 0.976\ NO_3^- + 2.90\ H_2O + 1.86\ CO_2 \quad (1)$$

Partial nitritation:

$$1\ NH_4^+ + 0.79\ O_2 + 1.14\ HCO_3^- \rightarrow 0.10\ C_5H_7NO_2 + 0.42\ NH_4^+ + 0.56\ NO_2^- + 1.08\ CO_2 + 1.68\ H_2O \quad (2)$$

ANAMMOX:

$$1\ NH_4^+ + 1.32\ NO_2^- + 0.066\ HCO_3^- + 0.13\ H^+ \rightarrow 1.02\ N_2 + 0.26\ NO_3^- + 0.066\ CH_2O_{0.5}N_{0.15} + 2.03\ H_2O \quad (3)$$

In comparison with the two-stage process using two separate reactors for PN and ANAMMOX, autotrophic single-stage nitrogen removal (ASNR) removes nitrogen in a single reactor by co-culturing AAOB and AnAOB. ASNR is cost-effective because of the small energy footprint and low capital cost [1, 2]. However, the acclimation of the activity of the AAOB and AnAOB is the most critical process in the start-up stage of ASNR. As an effective start-up strategy, poly(vinyl) alcohol/sodium alginate (PVA/SA) beads have been applied for ASNR previously [3]. Instead of a homogeneous gel structure, a core-shell structured gel bead effectively protects the AnAOB by entrapping AAOB in the shell layer [4]. Natural and synthetic polymers have been used for interfacial gelling to

Received March 1, 2018 **Accepted** September 3, 2018

† Corresponding author
Email: hyokwan.bae@pusan.ac.kr
Tel: +82-51-510-2392 Fax: +82-51-514-9574

fabricate the core-shell structure [4, 5]. In the interfacial gelling procedure, a core bead containing a gelling agent is immersed in a polymer solution. Afterward, the gelling agent in the core bead diffuses towards the polymer solution to promote the cross-linking reaction and construct the shell layer on the core bead.

In wastewater treatment processes, the core-shell structure exhibits a gradient of oxidative and reductive potentials because of the different concentrations of dissolved oxygen (DO) at different depths. Generally, the shell layer has a high oxidative potential because it faces a high concentration of DO in the bulk phase. In this study, shell layer provides the oxidative potential to AAOB for PN. In addition to active PN reaction, it is essential that DO should be consumed entirely by the AAOB to prevent the oxygen inhibition of AnAOB in the core bead. In a previous study, the shell layer immobilizing the AAOB was found to have a certain depth where oxygen penetrates, ranging from 0.067 to 0.967 mm; this effectively protects the AnAOB from oxygen inhibition by depleting DO via active ammonia-oxidizing activity [4]. As a result, the continuous mode ASNR showed a nitrogen removal rate of 590 g-N/m^3-d because of the cooperative activities of the AAOB and AnAOB in aerobic conditions [4]. Artificial nitrifying biofilms are a promising alternative to natural biofilms for rapid start-up of ASNR.

Although the feasibility of the core-shell structured PVA/SA gel beads has been proven for biological wastewater treatment, the low mechanical strength of PVA/SA may lead to the destruction of the shell layer and consequent loss of the AAOB biomass during the ASNR process. In addition, the toxic effect of free ammonia (FA) inhibits respiratory activity and potentially results in AnAOB inhibition due to the increased oxygen penetration depth. Therefore, in this study, the effects of PVA concentration, cross-linking reaction time, and nitrifying biomass concentration on the mechanical stability of the beads were investigated. The oxygen penetration depth, which is the critical parameter in the protection AnAOB, was verified using a microelectrode system under different DO and FA conditions.

2. Materials and Methods

2.1. Fabrication of the Shell Layer

The shell layer of the core-shell structured PVA/alginate beads was fabricated following the method shown in Fig. S1. Saturated $B(OH)_3$ and 1% $CaCl_2$ were used as gelling agents for PVA and SA, respectively [6]. The nitrifying biomass to be immobilized in the shell layer was obtained from a bench scale nitrifying reactor with an ammonium conversion rate of 0.8 kg-N/m^3-d with 99% nitrifying efficiency. The experimental conditions are summarized in Table 1. The first experiment was conducted with PVA concentrations of 7.5%, 10%, and 12.5% (No. 1 in Table 1). For the gelling method used in this study, a PVA concentration higher than 15% resulted in the irregularly shaped beads due to the high viscosity (data not shown). In the next step, interfacial gelling reaction times of 10, 30, 50, and 70 min were tested at a PVA concentration of 7.5% (No. 2 in Table 1). The nitrifying biomass concentration, which is the primary factor for the initial ammonia-oxidation activity, changed from 765 to 4,219 mg-VSS/L (No. 3 in Table 1). To measure the thickness of the shell layer, the beads were stored at −70℃ for 30 min and cut into two pieces at the center. The morphology of the shell layer is shown in Fig. S2. The gelling conditions are the same as Fig. S1 if not otherwise noted.

2.2. Measurement of the Mechanical Strength of the Shell Layer

Previously, the mechanical strength of the shell layer has been measured as the force required to burst the core-shell structured beads [5]. Carrageenan, chitosan, and alginate require a force of 5 N/bead to burst the beads, but the force required to burst beads containing 8% PVA has not been identified because of the high mechanical strength of PVA [5]. Therefore, in this study, the mechanical strength of the shell layer was measured using a high-speed agitation unit with four blades (4 cm in length and 2 cm in width) (Fig. S3). The internal diameter of the cylinder was 14 cm. A rapid agitation speed of 1,000 rpm was applied for 10 min. This procedure provides rapid and easy identification of the deformation of core-shell structured beads. Before the test, distilled water was added up to 10 cm from the bottom of the container, together with the core-shell structured beads. The number of beads that survived at the various agitation speed was counted to compare the mechanical strength of the shell layer. The tests were carried out in triplicate.

2.3. Distribution of Dissolved Oxygen in the Shell Layer

An oxygen microsensor (USOX-50, Unisense, Denmark) was loaded into the micromanipulator (USMC-232, Unisense, Denmark) to measure the DO concentration in the shell layer, and a step size of 50 μm was used. A holding unit to fix the bead at a certain position in the culture medium was designed (Fig. S4). The culture medium contained 100 mg-N/L $(NH_4)_2SO_4$ and 343 mg-C/L $NaHCO_3$. The mineral components were 6 mg-P/L KH_2PO_4,

Table 1. The Experimental Conditions for the Fabrication of the Shell Layer

No.	PVA concentration	Interfacial gelling reaction time	Nitrifying biomass concentration
1	7.5, 10, and 12.5%	30 min	2,321 mg-VSS/L
2	7.5%	10, 30, 50, and 70 min	1,572 mg-VSS/L
3	12.5%	30 min	765 mg-VSS/L 1,514 mg-VSS/L 2,888 mg-VSS/L 4,219 mg-VSS/L

12 mg-Mg/L $MgSO_4 \cdot 7H_2O$, and 48 mg-Ca/L $CaCl_2 \cdot 2H_2O$. Additionally, 1 mL/L of each trace element solutions were added to the influent. Trace element solution I consisted of 5 g/L EDTA and 5 g/L $FeSO_4 \cdot 7H_2O$. Trace element solution II consisted of 5 g/L EDTA, 0.43 g/L $ZnSO_4 \cdot 7H_2O$, 0.24 g/L $CoCl_2 \cdot 6H_2O$, 0.99 g/L $MnCl_2 \cdot 4H_2O$, 0.25 g/L $CuSO_4 \cdot 5H_2O$, 0.22 g/L $Na_2MoO_4 \cdot 2H_2O$, 0.19 g/L $NiCl_2 \cdot 6H_2O$, 0.21 g/L $Na_2SeO_4 \cdot 10H_2O$, and 0.014 g/L H_3BO_3. Before the measurement, the DO concentration of the culture medium was adjusted by balancing the ambient air and Ar purging intensities at the bottom of the solution. The DO concentrations were recorded by using logging software (SensorTrace PRO, version 3.1.3, Unisense, Denmark). The DO penetration depth was determined from the distance between the surface and the position exhibiting a DO of less than 0.2 mg/L, which is the detection limit of the microelectrode system.

2.4. Oxygen Uptake Rate

The respiratory activity of the AAOB was measured from the oxygen uptake rate (OUR) using a DO probe (YSI Model-58, USA). The culture medium for AAOB contained 100 mg/L NH_4^+-N and 171 mg/L HCO_3^--C. The base medium was the same as that in Section 2.3. The solution for the AAOB was purged with ambient air for 30 min to saturate the solution with DO. The slope of the decrease in DO concentration was calculated and used as an indicator of the AAOB activity.

2.5. Free Ammonia

The FA concentrations were calculated according to Eq. (4) and (5). A loading of 3,524 ± 241 mg-VSS/L of nitrifying biomass was entrapped in the shell layer. For FA concentrations, pH values of 6, 7, and 9 were applied at different NH_4^+-N concentrations of 250 and 400 mg/L at 25℃ and 8.0 mg/L of DO in the bulk phase.

$$NH_4^+ + OH^- \leftrightarrow NH_3 + H_2O \quad (4)$$

$$[NH_3\text{-}N]_{free} = \frac{[TAN] \cdot 10^{pH}}{\left(K_a/K_w\right) + 10^{pH}} \quad (5)$$

Here, TNA is the total ammonia nitrogen (ammonium + free ammonia (mg-N/L)), the ionization constant for ammonium per water [*Ka*/*Kw*] is $e^{6334/(273 + t)}$, *Ka* is the ionization constant for ammonia, *Kw* is the ionization constant for water, and *t* is the temperature in ℃.

3. Results and Discussion

3.1. Thickness

The thickness of the shell layer was proportional to the PVA concentration at a fixed gelling reaction time of 30 min in the range of 2.68-3.28 mm (Fig. S5(a)). During the gelling procedure, $B(OH)_3$ and $CaCl_2$, which diffuse out of the core bead, are limiting reagents in comparison to the large amount of PVA/SA in the bulk phase. Thus, the complete consumption of the gelling agents of $B(OH)_3$ and $CaCl_2$ would terminate the interfacial gelling reaction in a short-term period. To verify this, various reaction times of the interfacial gelling reaction were used (Fig. S5(b)). It was found that the reaction time was positively correlated with the thickness of the shell layer at a PVA concentration of 7.5%. Thus, the gelling reaction is a relatively slow process in the range of 10-70 min and significant time is required to reach a thickness of 2.01-2.70 mm. The nitrifying biomass loading also showed a positive relationship with the thickness between 2.77 and 3.63 mm (Fig. S5(c)). By using the positive relationship, the three factors can be used to extend the anaerobic zone of the core-shell structured gel beads to protect the AnAOB for ASNR.

3.2. Enhancement of Mechanical Strength

Generally, ASNR requires a DO concentration in the range of 0.2-1.0 mg/L [7, 8]. If the bead loses the shell layer, the AnAOB are immediately exposed to an inhibitory DO concentration. Note that the inhibitory DO concentration for AnAOB is in the range of 0.08 to 1.44 mg/L [9]. Therefore, the high mechanical strength of the shell layer is a critical property ensuring the stability of the ANAMMOX reaction for ASNR.

In this study, it was hypothesized that the mechanical strength is proportional to the thickness of the PVA/SA layer. At a 7.5% PVA concentration with 2.68 mm thickness, all the core-shell structured beads were broken at an agitation rate of 1,000 rpm (Fig. 1). In contrast, at PVA concentrations of 10% and 12.5% with increased thicknesses of 2.96 and 3.28 mm, respectively, 12.3% and 62.1% of the double-layered gel beads survived. Therefore, the mechanical strength of the shell layer seems to be correlated with the thickness. However, the positive correlation was not valid when the interfacial gelling reaction time and nitrifying biomass concentration were independent variables. All the beads with different interfacial gelling reaction time at a 7.5% PVA concentration were broken, regardless of the thickness variation (data not shown). Likewise, there was little difference in mechanical strength with varying nitrifying biomass concentration (Fig. 2). In conclusion, the PVA concentration is the predominant control factor determining the mechanical strength of the shell layer, and a high PVA concentration is preferable to maintain

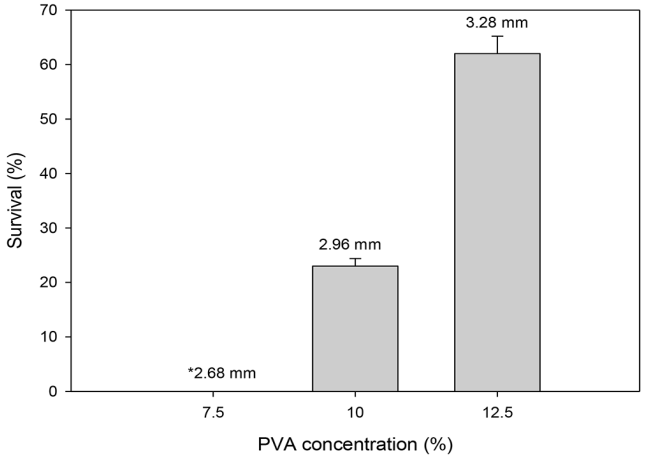

Fig. 1. Effects of PVA concentration on the survival ratio of the shell layer at a fast agitation rate of 1,000 rpm. (*Thickness of the shell layer is indicated.)

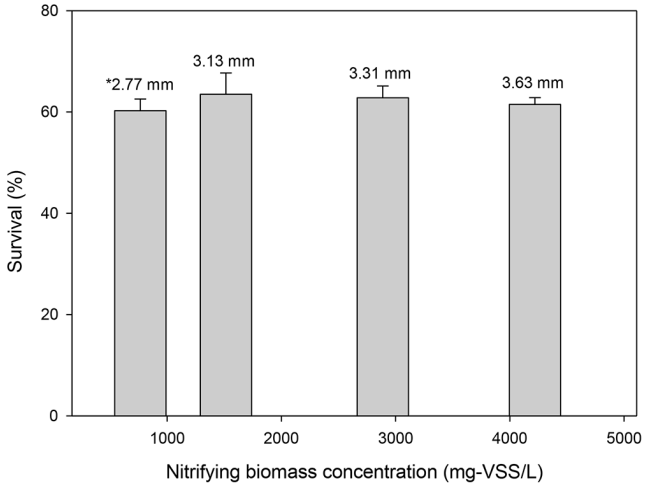

Fig. 2. Effects of nitrifying biomass concentration on the survival ratio of the shell layer at a fast agitation rate of 1,000 rpm. (*Thickness of the shell layer is indicated.)

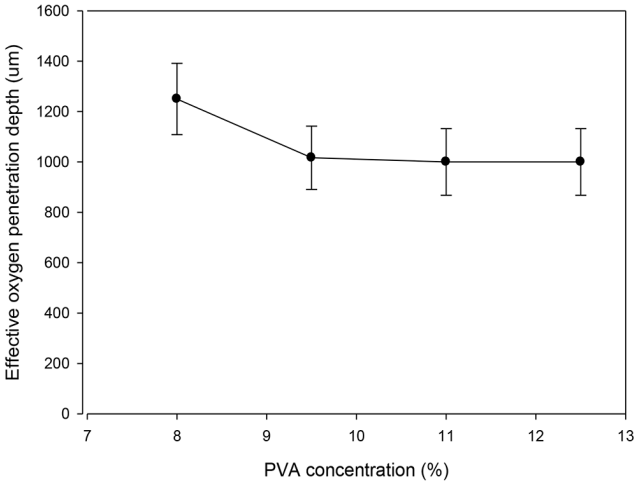

Fig. 3. The effect of PVA concentrations on the oxygen penetration depth.

high mechanical strength. Note that a dense PVA/SA structure can result in the slow diffusion of ammonium and oxygen, consequently reduces the respiration of AAOB. Thus, the oxygen penetration depth was determined at different PVA concentrations.

3.3. The Effect of Dissolved Oxygen in the Bulk Phase on the Oxygen Penetration Depth

A previous study reported that the PVA/SA shell layer for ASNR effectively protects AnAOB when the oxygen penetration depth is 0.067 to 2.35 mm, but this mainly depends on the nitrifying biomass concentration [4]. However, there is limited knowledge of the effect of PVA concentration on the oxygen penetration depth. In this study, 8.0%, 9.5%, 11.0%, and 12.5% PVA concentrations were applied to measure the oxygen penetration depth at a DO concentration of 8.0 mg/L (Fig. 3). The shell layer contained a nitrifying biomass of 2,064 ± 28 mg/L. An 8.0% PVA concentration resulted in oxygen diffusion of up to 1.25 mm, while other higher PVA concentrations resulted in a 20% reduction in the oxygen penetration depth to 1.0 mm.

The DO in the bulk phase is the primary factor determining the oxygen penetration depth and the aerobic ammonia-oxidation activity. In the case of DO control failure, a high DO concentration in the bulk phase can result in a greater oxygen penetration depth. In this study, the oxygen penetration depth was measured for DO concentrations of 0.6, 2, 5, and 8 mg-DO/L in the bulk phase for 8.0% and 12.5% PVA concentrations with 2,441 ± 238 mg-VSS/L of nitrifying biomass (Fig. 4). The oxygen penetration depth increased with increasing DO concentration in the bulk phase. At 12.5% PVA concentration, the maximum oxygen penetration depth at 8.0 mg-DO/L was 1.0 mm, whereas an extended oxygen penetration depth of 1.25 mm for 8.0% PVA concentration was observed. However, no differences in the oxygen penetration patterns were observed for DO concentrations of 0.6, 2, and 5 mg/L between PVA concentrations of 8% and 12.5%. In conclusion, the PVA concentration controls the thickness of the shell layer, but its effect on the oxygen penetration depth is almost negligible.

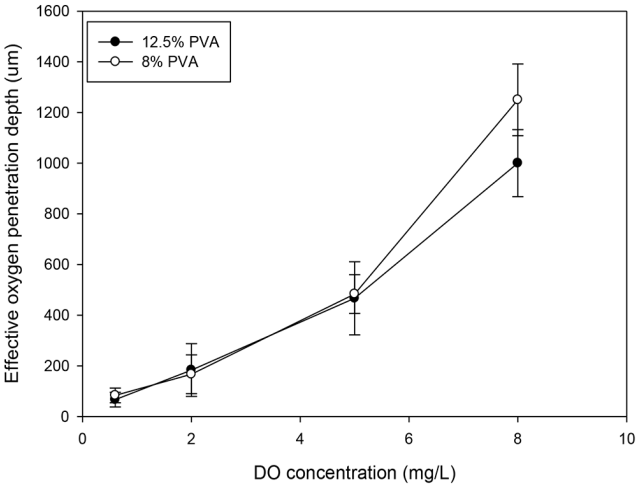

Fig. 4. The effect of DO and PVA concentrations on the oxygen penetration depth.

In this study, shell layers of more than 2.0 mm were fabricated by various gelling procedures. Considering the oxygen penetration depth ranging from 0.083 to 1.25 mm shown in Fig. 4, it was expected that the shell layer would effectively protect ANAMMOX bacteria from oxygen, even if the bulk phase was saturated with DO.

3.4. Effect of Free Ammonia

The presence of FA selectively inhibits the nitrite-oxidizing bacteria (NOB) activity at 0.1-1.0 mg/L < FA < 10-150 mg/L [10]. However, an FA concentration of more than 150 mg/L causes inhibition of AAOB activity. In this situation, oxygen penetrates the shell layer to a significant extent. To verify the extended oxygen penetration depth, various FA concentrations were applied to the entrapped AAOB in the shell layer. In addition, for the effect of the entrapment, the suspended nitrifying biomass was exposed to different FA concentrations (Fig.

S6). For AAOB in the suspended growth phase, FA concentrations of more than 13 mg/L significantly inhibited the respiratory activity.

As a control experiment, AAOB biomass was not added to the shell layer. A previous study showed a linear relationship between the AAOB biomass concentration and the oxygen penetration depth because of the active respiration of the AAOB [4]. However, in this study, the oxygen penetration depth without respiration activity could not be determined due to the effective penetration of oxygen in the porous PVA/SA hydrogel structure. The oxygen profile in Fig. 5 shows a consistent oxygen concentration of 8.3 mg/L throughout the shell layer, regardless of depth.

The effects of the physiochemical properties of PVA/SA hydrogel are still questionable. At the steady-state, the balance between respiration activity and oxygen diffusion rate controls the oxygen penetration depth. It was found that the oxygen diffusivities are 1.6-2.0 $\times$ 10^{-9} and 2.83 $\times$ 10^{-9} m^2/s for natural polymers and water, respectively [11]. In comparison, PVA/SA showed a relatively low oxygen diffusivity of 1.5 $\times$ 10^{-9} m^2/s [11]. However, detailed information concerning the effect of physiochemical properties of PVA/SA on the oxygen diffusivity is not available. Thus, further intensive investigation is required concerning the oxygen diffusion at various PVA concentrations, shell thicknesses, and AAOB biomass concentrations.

A reduction in the oxygen concentration through the shell layer was clear after the entrapment of nitrifying biomass at a concentration of 3,524 ± 241 mg-VSS/L. In the presence of 400 mg-N/L of NH_4^+ and 0 mg-FA/L at pH 6, the oxygen penetration was 2,900 μm because of the lack of FA substrate and consequent low respiratory activity. However, the oxygen penetration depth was drastically reduced to 900 μm at pH 7 with 1.7 mg-FA/L. AAOB respiration was activated at higher FA concentrations because ammonia is considered the substrate for AOB rather than ammonium [12]. Likewise, a higher FA concentration of 176.0 mg-FA/L resulted in a similar oxygen penetration depth of 850 μm.

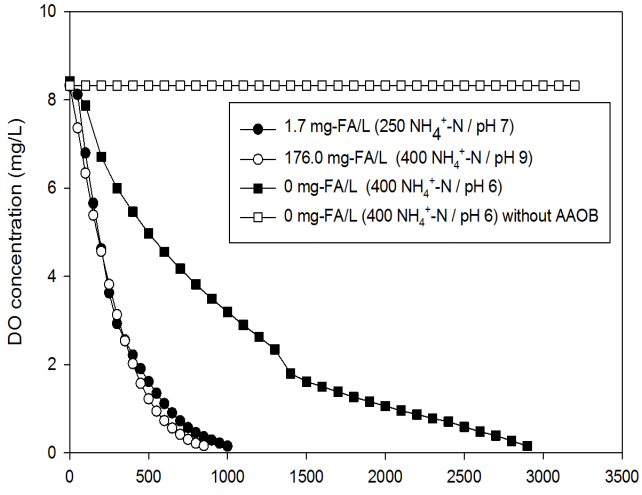

Fig. 5. Vertical distribution of oxygen through the shell layer at various FA concentrations

The results obtained for immobilized AAOB contradict the results obtained with suspended AAOB at higher FA concentrations; that is, only 20 mg-FA/L can inhibit the respiration activity of suspended AAOB (Fig. S6). It was expected that the protective effect of immobilization in the PVA gel layer would result in a favorable environment for AAOB, even at high FA concentrations. In the same manner, it was demonstrated that the immobilized AAOB cells are 30% less sensitive to FA stress [13]. However, further in-depth investigation is required to reveal the protective effects of the entrapment of AAOB in the PVA/SA matrix under FA stress.

4. Conclusions

The structural stability and oxygen penetration depth of the PVA/SA shell layer were successfully characterized in this study. The mechanical strength of the shell layer depends on the PVA concentration, and a 12.5% PVA was the optimum concentration for the enhancement of the mechanical stability of the core-shell structured gel bead. The oxygen penetration depth was affected by the PVA concentration, DO concentration in the bulk phase, and FA concentration. Under appropriate ammonia concentrations, the oxygen penetration depth was around 1,000 μm when sufficient oxygen was supplied from the bulk phase, such as 8.0 mg-DO/L. Therefore, the shell layer with the thickness in the range of 2.01-3.63 mm can effectively protect ANAMMOX bacteria in the core beads from the oxygen inhibition in ASNR.

Acknowledgments

This project was supported by the "R&D Center for Reduction of Non-CO_2 Greenhouse Gases (2017002420003)" funded by Korea Ministry of Environment (MOE) as "Global Top Environment R&D Program."

This article was presented at the 2017 International Environmental Engineering Conference (IEEC2017) held on 15-17 November 2017, Jeju, Korea.

References

1. Varas R, Guzmán-Fierro V, Giustinianovich E, Behar J, Fernández K, Roeckel M. Startup and oxygen concentration effects in a continuous granular mixed flow autotrophic nitrogen removal reactor. *Bioresour. Technol.* 2015;190:345-351.
2. Vlaeminck SE, De Clippeleir H, Verstraete W. Microbial resource management of one-stage partial nitritation/anammox. *Microb. Biotechnol.* 2012;5:433-448.
3. Qiao S, Tian T, Duan X, Zhou J, Cheng Y. Novel single-stage autotrophic nitrogen removal via co-immobilizing partial nitrifying and anammox biomass. *Chem. Eng. J.* 2013;230:19-26.
4. Bae H, Choi M, Chung YC, Lee S, Yoo YJ. Core-shell structured poly(vinyl alcohol)/sodium alginate bead for single-stage autotrophic nitrogen removal. *Chem. Eng. J.* 2017;322:408-416.
5. dos Santos VAM, Vasilevska T, Kajuk B, Tramper J, Wijffels

RH. Production and characterization of double-layer beads for coimmobilization of microbial cells. *Biotechnol. Annu. Rev.* 1997;3:227-244.
6. Bae H, Yang H, Choi M, Chung YC, Lee S, Yoo YJ. Optimization of the mechanical strength of PVA/alginate gel beads and their effects on the ammonia-oxidizing activity. *Desalin. Water Treat.* 2015;53:2412-2420.
7. Helmer C, Tromm C, Hippen A, Rosenwinkel KH, Seyfried CF, Kunst S. Single stage biological nitrogen removal by nitritation and anaerobic ammonium oxidation in biofilm systems. *Water Sci. Technol.* 2001;43:311-320.
8. Chang XY, Li D, Liang YH, et al. Performance of a completely autotrophic nitrogen removal over nitrite process for treating wastewater with different substrates at ambient temperature. *J. Environ. Sci.-China* 2013;25:688-697.
9. Egli K, Fanger U, Alvarez PJ, Siegrist H, Van der Meer JR, Zehnder AJ. Enrichment and characterization of an anammox bacterium from a rotating biological contactor treating ammonium-rich leachate. *Arch. Microbiol.* 2001;175:198-207.
10. Bae H, Yang H, Chung YC, Yoo YJ, Lee S. High-rate partial nitritation using porous poly(vinyl alcohol) sponge. *Bioprocess Biosyst. Eng.* 2014;37:1115-1125.
11. Leenen EJ, Dos Santos VA, Grolle KC, Tramper J, Wijffels R. Characteristics of and selection criteria for support materials for cell immobilization in wastewater treatment. *Water Res.* 1996;30:2985-2996.
12. Prosser JI. Autotrophic nitrification in bacteria. *Adv. Microb. Physiol.* 1990;30:125-181.
13. Yan J, Hu YY. Partial nitrification to nitrite for treating ammonium-rich organic wastewater by immobilized biomass system. *Bioresour. Technol.* 2009;100:2341-2347.